ON THE FRACTURE OF NUCLEAR REACTOR TUBES

By

E. S. Folias

University of Utah
Department of Civil Engineering
Salt Lake City, Utah
U. S. A.

1. Introduction

In general, fracture in nuclear reactor tubes is initiated by some flaw or imperfection, such as a microcrack, which induces high stresses in that vicinity. For a sufficiently high value of the local stress, the atomic bonds at the crack edge may be broken. When this happens, the flaw may grow into a sizable fracture surface, thus causing complete failure of the structure. To ensure, therefore, the integrity of the structure, the designer must be cognizant of the relation that exists among fracture load, flaw shape and size, material properties, and structural geometry. A relation of this kind is called a fracture criterion and can be derived by the application of the theory of fracture mechanics.

For the derivation of a fracture criterion two ingredients are necessary: (i) a knowledge of the stress distribution due to the presence of a crack, and (ii) an energy balance for crack initiation.

2. The Stress Field in the Vicinity of the Crack

Let us consider a portion of a thin, shallow* cylindrical shell of constant thickness h and subjected to a uniform internal pressure q_o. The material of the shell is assumed to be homogeneous and isotropic and that the deformations are small so that the stress-strain relations may be established through Hooke's Law.

The basic variables in the theory of shallow shells are the displacement function $w(x,y)$ in the direction of the z-axis and a stress function $F(x,y)$ which represents the stress resultants tangent to the middle surface of the shell. Following Marguerre [1], the coupled differential equations governing W and F for a cylindrical shell, with x and y as rectangular cartesian coordinates of the base plane, are given by

$$\frac{Eh}{R}\frac{\partial^2 W}{\partial x^2} + \nabla^4 F = 0 \tag{1}$$

$$\nabla^4 W - \frac{1}{RD}\frac{\partial^2 F}{\partial x^2} = -\frac{q_o}{D}, \tag{2}$$

where ∇^4 is the biharmonic operator, E Young's modulus, D the flexural rigidity and R the radius of the shell or tube.

Two cases of special practical interest immediately come to mind**: a tube with an axial crack and a tube with a peripheral crack. Both problems have been investigated by the author and the results can be found in references [2] and [3] respectively. Thus, without going into the mathematical details, the stress distribution around the crack tip is found to be

Extensional stresses: through the thickness

$$\sigma_x^{(e)} = P^{(e)}\sqrt{(c/2r)}\left(\frac{3}{4}\cos\frac{\theta}{2} + \frac{1}{4}\cos\frac{5\theta}{2}\right) + 0(r^0) \tag{3}$$

$$\sigma_y^{(e)} = P^{(e)}\sqrt{(c/2r)}\left(\frac{5}{4}\cos\frac{\theta}{2} - \frac{1}{4}\cos\frac{5\theta}{2}\right) + 0(r^0) \tag{4}$$

$$\tau_{xy}^{(e)} = P^{(e)}\sqrt{(c/2r)}\left(-\frac{1}{4}\sin\frac{\theta}{2} + \frac{1}{4}\sin\frac{5\theta}{2}\right) + 0(r^0) \tag{5}$$

---

* A shell is shallow if the radius of curvature is greater by one order of magnitude than the linear dimensions, i.e., L/R ≤ 0.1 and thin if h/R ≤ 0.01 .
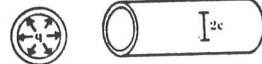
** For an arbitrarily oriented crack see reference [4].

Bending stresses:

$$\sigma_x^{(b)} = P^{(b)}\frac{z}{h}\sqrt{(c/2r)}\left(-\frac{3-3\nu}{4}\cos\frac{\theta}{2}-\frac{1-\nu}{4}\cos\frac{5\theta}{2}\right)+0(r^0) \tag{6}$$

$$\sigma_y^{(b)} = P^{(b)}\frac{z}{h}\sqrt{(c/2r)}\left(\frac{11+5\nu}{4}\cos\frac{\theta}{2}+\frac{1-\nu}{4}\cos\frac{5\theta}{2}\right)+0(r^0) \tag{7}$$

$$\tau_{xy}^{(b)} = P^{(b)}\frac{z}{h}\sqrt{(c/2r)}\left(-\frac{7+\nu}{4}\sin\frac{\theta}{2}-\frac{1-\nu}{4}\sin\frac{5\theta}{2}\right)+0(r^0). \tag{8}$$

where r, θ are the usual cylindrical coordinates with center at the crack tip, 2c the length of the crack and ν Poisson's ratio. Furthermore, the stress coefficients $P^{(e)}$ and $P^{(b)}$ are functions of the radius of the tube, the crack to thickness ratio, the material properties and finally the external loading. While the true expressions are rather lengthy (see reference [4]), for long tubes they may be approximated within a 6% error by the following simple relations:*

Long cylinder axial crack	$P^{(e)} \approx q_0\sqrt{1+0.317\lambda^2}\ \dfrac{R}{h}$ $P^{(b)} \approx 0$
Long cylinder peripheral crack	$P^{(e)} \approx q_0\sqrt{1+0.05\lambda^2}\ \dfrac{R}{2h}$ $P^{(b)} \approx 0$.

(9)

where
$$\lambda^4 \equiv \frac{12(1-\nu^2)}{R^2 h^2} c^4 . \tag{10}$$

3. Fracture Criterion

3.1 Elastic Considerations

From the foregoing discussion, it becomes apparent that tubes containing through cracks present a reduced resistance to fracture initiation. Consequently, the presence of a crack in the walls of a pressure tube can severely reduce the strength of the structure and can cause sudden failure at nominal tensile stresses less than the material yield strength.

Thus following the work of Griffith [5], we derive the following fracture criterion for crack instability

$$4\gamma c = \frac{2}{E}\pi c\left\{\left[P^{(e)}\right]^2 + 2\frac{\pi}{E}c^2\ P^{(e)}\left[\frac{dP^{(e)}}{dc}\right]\right\} \tag{11}$$

where γ is the surface energy per unit area.

3.2 Plastic Considerations

Due to the presence of high stresses in the vicinity of the crack tip, when the appropriate yield criterion is satisfied then localized plastic deformation occurs and a plastic zone size is created. This phenomenon effectively increases the crack length and therefore must be accounted for. Thus following Dugdale [6], one derives the following fracture criterion which includes plasticity and geometry conditions

$$P^{(e)} = \frac{2\sigma^*}{\pi}\cos^{-1}\left[\exp\left(-\frac{\pi K^2}{8\sigma^{*2}c}\right)\right], \tag{12}$$

---
* The reader should notice that for very long cracks $P^{(b)} \approx 0$. Also in such cases bulging effects can no longer be neglected.

where K represents the fracture toughness of the material and

$$\sigma^* = \frac{3}{4}\sigma_y + \frac{1}{4}\sigma_u \tag{13}$$

with σ_y and σ_u being the yield and ultimate stress respectively.

4. <u>Experimental Verification</u>

In judging the adequacy of a theory, one often compares theoretical and experimental results. Therefore, in the following we compare our results with some of the experimental data existing in literature.

1. "Additional Crack Propagation Tests on Zircaloy-2 Pressure Tubes," R.C. Aungst. Electro-technical Technology, Vol. 4, No. 7-8, July/August 1966.

Results of tests on 2.7" diameter, 0.26" thick N-Reactor tube with v-shape cracks.

Material: 30% cold drawn zircaloy-2.

σ_y: 98 ksi $\sigma^* = 98.4$ ksi

σ_u: 98.6 ksi $k = 240$ ksi$\sqrt{\text{in}}$

The results are plotted in Figure 1. Notice that the agreement is very good for large crack lengths. However, for small crack lengths the predicted values are somewhat lower. This is not contrary to our expectations for our calculations were based on through the thickness cracks.

2. "Fracture Mechanics of Through-Cracked Cylindrical Pressure Vessels," R. B. Anderson, T. L. Sullivan. NASA TN D-3252.

Results of tests on 6" diameter, 0.060" thick cylinders with full thickness cracks.

a) Material: 2014-T6Al

σ_y 90.5 ksi $\sigma^* = 91.9$ ksi

σ_u 93.9 ksi $k = 51.6$ ksi$\sqrt{\text{in}}$

The results are plotted in Figure 2. The agreement is good.

b) Material: 2014-T6Al

σ_y: 82.0 ksi $\sigma^* = 85.0$ ksi

σ_u: 93.9 ksi $k = 48.6$ ksi$\sqrt{\text{in}}$

The results are plotted in Figure 3. The agreement is good.

3. "Fast Fracture of Pressure Vessels" An Appraisal of Theoretical and Experimental Aspects and Application to Operational Safety," W. H. Irvine, A. Quirk and E. Bevitt. Journal British Nuclear Energy Society, January 1964.

The results of tests on 5' diameter, 1" thick, cylindrical vessels with through cracks.

Material: 0.36% C Steel

σ_y: 33 ksi $\sigma^* = 40$ ksi

σ_u: 61 ksi $k = 179$ ksi$\sqrt{\text{in}}$

The results are plotted in Figure 4. The agreement is fairly good.

5. <u>Effect of Thickness</u>

A major debility in current fracture mechanics work is the ignorance of the effects of thickness on the mechanism of failure. For example, the common experimental observation of a change from ductile failure at the edge to brittle fracture at the center of a broken sheet material has so far defied analysis.

Recently, however, the author was able to study the three-dimensional stress field in a plate of an arbitrary (finite) thickness 2h, and the results are reported in

reference [7]. In summary, it was found that (i) in the interior layers of the plate the stresses possess the usual $\frac{1}{\sqrt{r}}$ singular behavior with the stress intensity factor now being an increasing function of z (ii) in the neighborhood of the corner point all stresses are proportional to $\rho^{-1/2 - 2\nu}$, where ρ now is the spherical radius with center the corner point.

Furthermore, one can show that the through-the-thickness crack initiates at the center and takes the form of a bell shape curve*. The total strain energy was then computed for various crack-to-thickness ratios and the two well known limits of plane strain and plain stress were recovered. Finally, in order to derive a meaningful fracture criterion for thick plates, one must combine appropriately the two types of fracture. This matter is currently under investigation.

References

[1] Marguerre, K., Zur Theorie der Gekrummten Platte Grosser Formanderung, Proceedings of the 5th International Congress of Applied Mechanics, 93-101, (1938).

[2] Folias, E. S., International Journal of Fracture Mechanics, 1, 1, 20-46, (1965).

[3] Folias, E. S., International Journal of Fracture Mechanics, 3, 1, 1-11, (1967).

[4] Fung, Y. C. and Sechler, E. E., Thin Shell Structures, Prentice-Hall, Chapter 21, January 1974.

[5] Griffith, A. A., The Theory of Rupture, Proceedings of the 1st International Congress of Applied Mechanics, pp. 55-63, Delft, 1924.

[6] Dugdale, D. S., Journal of Mechanics and Physics of Solids, Vol. 8, p. 100, 1960.

[7] Folias, E. S., "On the Three-Dimensional Theory of Cracked Plates", to appear in the Journal of Applied Mechanics.

---

* We assume that $h > h_{crit.}$ so that normal fracture is possible. For $h \leq h_{crit.}$ the fracture is slant. The latter fracture is governed by the stress distribution of the corner point.
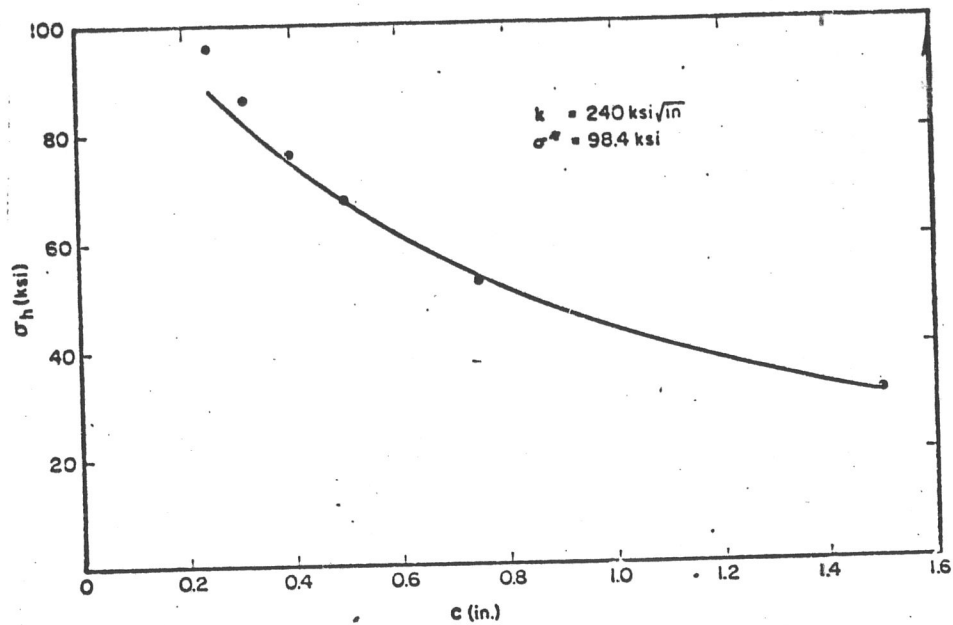
Fig. 1. Comparison between theory and experiment for
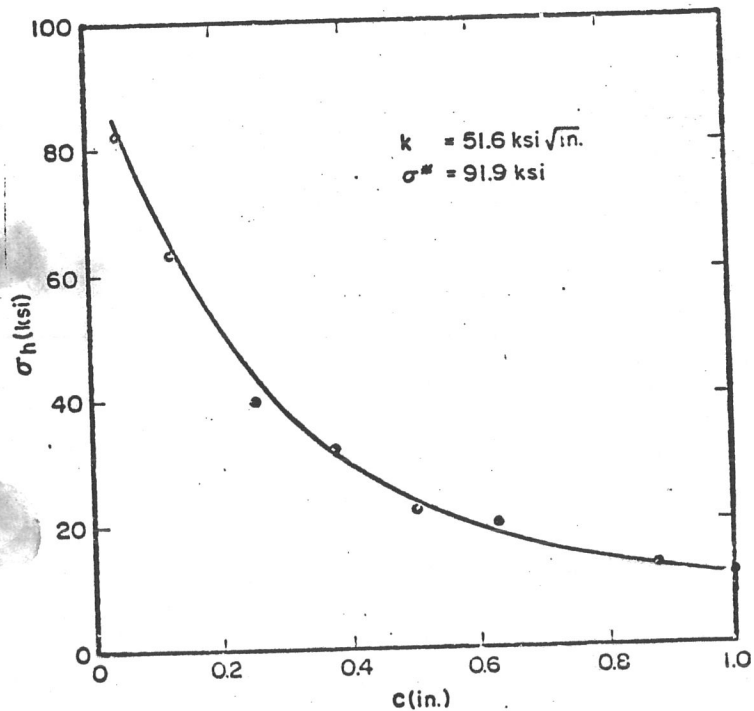30% zircaloy-2 N-reactor tubes with v-shape cracks.

Fig. 2. Comparison between theory and experiment for
2014-T6A1 cylindrical vessels at -423° F.
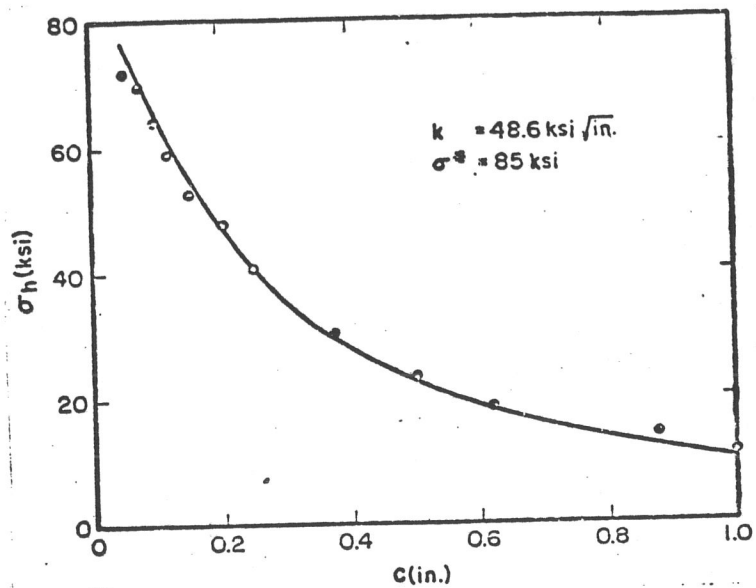
Fig. 3.   Comparison between theory and experiment for
          2014-T6Al cylindrical vessels at -320°F.
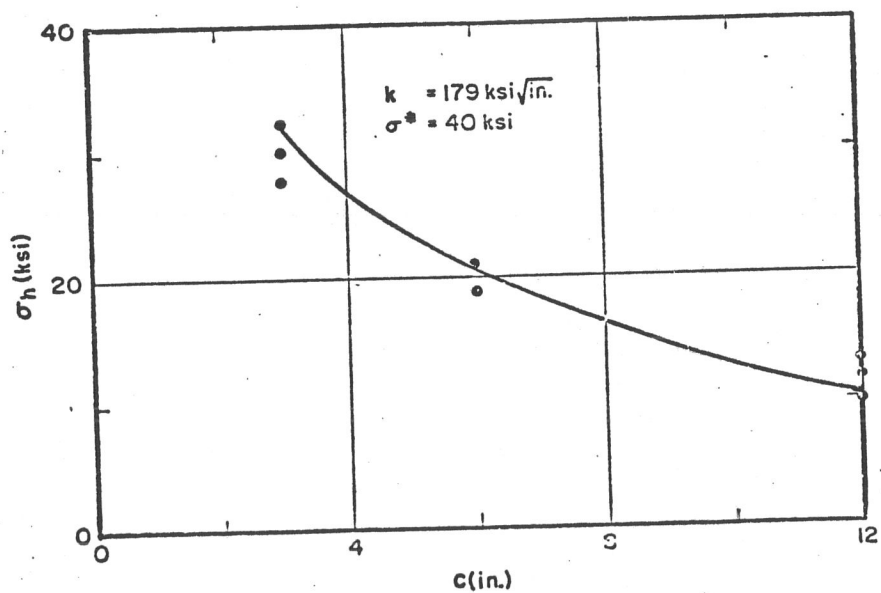

Fig. 4.   Comparison between theory and experiment for
          0.36% C steel cylindrical vessels.